ISSN: 0976-3376

Available Online at http://www.journalajst.com

ASIAN JOURNAL OF SCIENCE AND TECHNOLOGY

Asian Journal of Science and Technology
Vol. 08, Issue, 09, pp.5725-5729, September, 2017

RESEARCH ARTICLE

THIOLATED TRUXENE DERIVATIVES AS HOLE-TRANSPORTING MATERIALS FOR EFFICIENT PEROVSKITE SOLAR CELLS

***Anirban Pradhan**

Director's Research Unit, Indian Association for the Cultivation of Science, 2A & 2B,
Raja S. C. Mullick Rd, Jadavpur, Kolkata – 700032, India

ARTICLE INFO

Article History:
Received 08th June, 2017
Received in revised form
22nd July, 2017
Accepted 18th August, 2017
Published online 27th September, 2017

Key words:
Truxene, Perovskite solar cell (PSC),
Hole-transporting materials (HTMs),
Power conversion efficiency (PCE).

ABSTRACT

New C_3 symmetric star-shaped thiolated hole-transporting materials (HTMs) including a truxene core have been successfully synthesized and investigated for high performance perovskite solar cells. These findings open the opportunities for efficient HTMs based on the functionalized truxene utilizing the strong interactions of their functional groups with perovskite. Maximum power conversion efficiency (PCE) of 11.87 % has been achieved by employing thiolated truxene derivatives.

INTRODUCTION

Since the first reported in 2009 by Miyasaka, (Kojima, 2009), perovskite-based solar cells (PSCs) have great interest because of their unique optical and electrical properties and rapidly become the hottest topic in photovoltaics. The organic-inorganic hybrid perovskite solar cells (PSCs) have drawn great attentions as a real competitor to silicon solar cell, (Im*et al.*, 2012; Kim*et al.*, 2012; Lee, 2012; Zhou*et al.*, 2014; Zhou, 2015; Jeon, 2014; Yang, 2015; Mei, 2014 and Nie, 2015),due to their high power conversion efficiencies, easy fabrication, and low cost. Moreover, the organic-metal halide perovskites are direct band gap materials which exhibit strong light harvesting characteristics within the visible solar spectrum (Lim*et al.*, 2016). In PSCs, lead halide perovskite $CH_3NH_3PbI_3$ widely used as perovskite semiconductors, act as photo absorbers to generate free carriers that can be collected in the electrodes through both p- and n-type buffer layers (Yamada*et al.*, 2014; Manser, 2014 and La-o-vorakiat, 2015).PCEs in a relatively short period for such cells have been substantially increased, mainly improvements of the fabrication protocols for the perovskite layer (Xiao, 2014 and Ahn, 2015). However, a large amount of the converted photon energy is wasted by the surface recombination resulting from the imperfect crystal passivation and undesirable interfacial behaviour. Therefore, further efficiency enhancement mainly relies on minimizing the interface losses by interface modification within the active layers (Min, 2015).Recently, a breakthrough in PCE has been achieved by replacing traditional dyes with organic−inorganic hybrid perovskite (Min*et al.*, 2016; Liu*et al.*, 2015 and Zuo, 2015).The HTMs at the other side of perovskite layer also play an important role in the most efficient PSCs. Recently, an impressive PCEs was achieved over 18% with 5,10,15-trihexyl-3,8,13-tris(4-methoxyphenyl)-10,15-dihydro-5H diindolo[3,2-a:3′,2′-c]carbazole (triaza-truxene derivative) (Zhou, 2014) as an HTM. In these PSCs, triazatruxene (TAT) derivatives have been utilized to be an excellent HTM, even though other small-molecule HTMs such as 3, 4- ethylenedioxythiophene-, (Li*et al.*, 2014)pyrene-, (Jeon*et al.*, 2013)linear π-conjugated-, (Wang*et al.*, 2014) butadiene-, (Lv*et al.*, 2014)andspiro-OMeTAD derivatives-(Jeon, 2014)based HTMs, etc gave high conversion efficiencies of 11 to 20%. Some polymer HTMs (Xiao, 2014)with excellent electrical properties also resulted in high photovoltaic performances The development of alternative HTMs are left an attractive goal because they are cheaper and easier to purify than that of the spiro-OMeTAD. An ideal HTM generally requires compatible energy level, sufficient charge extraction and transferability.Zheng *et. al.* reported that introducing thiols unit into the hexabenzocoronene (TSHBC) (Cao, 2015), skeleton worked as a HTM for PSCs. Although it has poor hole mobilities which limit the fill-factor and thus overall efficiency of perovskite solar cells but larger intermolecular π-orbital overlap, improved stability, and ease of functionalization also. To the best of our knowledge, Zheng

---

****Corresponding author: Anirban Pradhan,***
Director's Research Unit, Indian Association for the Cultivation of Science, 2A & 2B, Raja S. C. Mullick Rd, Jadavpur, Kolkata – 700032, India

et al employed thiolatednanographenes (TSHBC) in PSCs as HTMs to date.

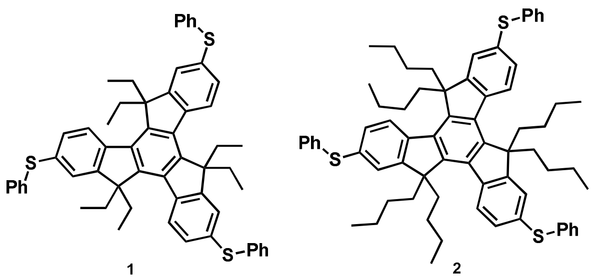

Scheme 1. Structures of synthesized star-shaped HTMs

Star-shaped truxene and triazatruxene derivatives are potential new HTMs for PSCs, since they have been known as hole selective layers for organic solar cells.Truxene has been used for nonlinear optical (NLO), organic photovoltaics (OPVs), and organic light-emitting diodes (OLEDs). Truxene core being structured from three indene units combined by one benzene ring can be considered as a two-dimensional π-system, which provides a large aromatic surface to overlap with each other for efficient intermolecular charge hopping. In addition, it offers large chemical versatility to tune electronic and morphological properties. Considering these advantages and high hole mobility values,herein, we use thiolated star shaped rigid plannar 10,15-30 dihydro-5*H*-diindeno[1,2-*a*;10,20-*c*]fluorine (truxene) (Scheme 1) as the HTMs in the pristine form in PSCs. The peripheral thiol groups form Pb−S coordination bonds at the interface of perovskite and HTM. The tight binding of thiolatedtruxene helps to rapidly extract charge from perovskite, resulting in a low energy loss at the interface. The performance is readily improved by doping with plannarthiolatedtruxene to enhance the hole transporting property within HTM.

The synthesis started from alkylations of the known 10,15-dihydro-5H-diindeno[1,2-a:1',2'-c]fluorine (truxene)3 (Scheme 2) with 1-bromoethane and 1-bromobutane respectively in the presence of KOH to give compounds 4a and 4b in a quantitative yield. Six alkyl groups were introduced to the truxene core to increase the solubility and also to increase their hydrophobicity. Compounds 4a and 4b was brominated with bromine in chloroform with a catalytic amount of $FeCl_3$ at 0 ^{o}C, giving compounds 5a and 5b respectively in a high yield. Compounds 5a and 5b was then treated with thiol and a catalytic amount of $[Pd(OAc)_2]$ to give 1(80%) and 2(75%) respectively (ESI), despite the three nucleophilic substitution reactions. The normalized UV−vis absorption spectra of 1 and 2 in DCM solution are shown in Figure 1a. Absorption bands appear in the spectral region between 250 and 350 nm, which are assigned to the π−π* transitions of the conjugated system. The experimental HOMO energy levels of the thiolatedtruxene derivatives were estimated from cyclic voltammogram with ferrocene as external reference (Figure 1b). The LUMO/HOMO values were determined as -5.95/-2.80 eV and -5.92 eV/-2.82 eV *vs* vacuum for 1 and 2, respectively (Table 1). The HOMO levels are slightly higher than that of $CH_3NH_3PbI_3$perovskite (-5.40 eV). The alkyl chains almost didn't influence their energy levels. To further understand their electronic structures, the molecular orbitals (MO) of thiolatedtruxene were calculated through the density functional theory (DFT) method at the B3LYP/6-311G(d,p) level in gas phase.

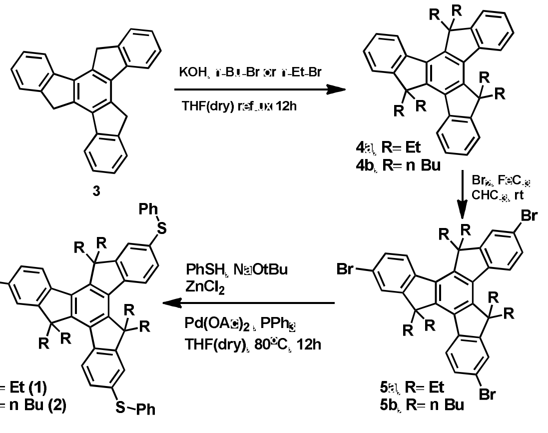

Scheme 2. Synthesis of thiolatedtruxene

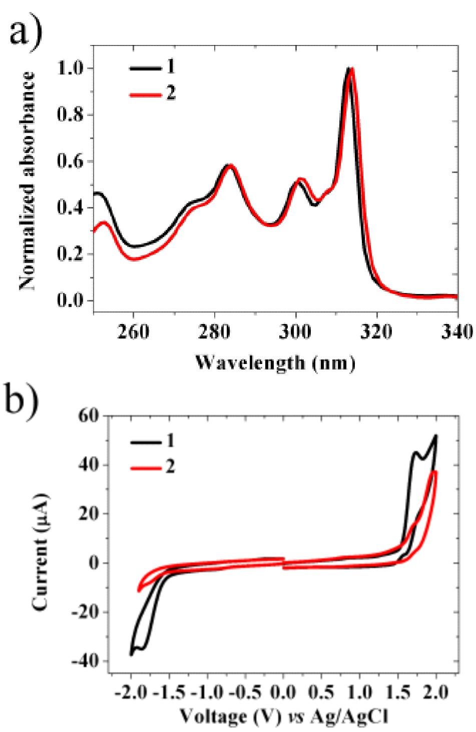

Figure 1. a) Normalized absorption spectra of 1 and 2 in CH_2Cl_2 (1×10^{-5} M). b) Cyclic voltammetry of 1 and 2 in CH_2Cl_2 with 0.1 M *n*-Bu4NPF_6 as the supporting electrolyte

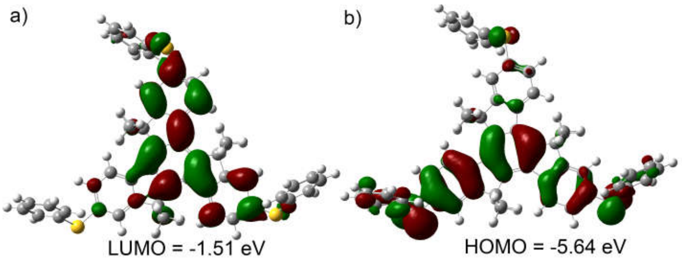

Figure 2. a), b) LUMO and HOMO of thiolatedtruxene optimized at the B3LYP/6-311G(d,p) level. Alkyl chains were replaced by methyl to facilitate the calculation

Alkyl chains were replaced by methyl. As shown in Figure 2, the introduction of thiophenyl influence both HOMO and LUMO of truxene derivatives due to the delocalization of HOMO and LUMO to thiophenyl. The planar and large π-conjugated backbone contribute to their ordered packing in solid state, thus enhance their carrier transport abilities.

Table 1. Summary of optical and electrochemical data

Entry	HOMO (eV)	LUMO (eV)	Eg (eV)
1	-5.95	-2.80	3.91
2	-5.92	-2.82	3.90

Compound **1** and **2** were used as HTMs. The PSCs had a typical p-i-n configuration of FTO/TiO_2/ $CH_3NH_3PbI_3$/ Thiolatedtruxene/Au. In a typical fabrication procedure, the compact TiO_2 layer and mesoporous TiO_2 layer were deposited on a FTO (fluorine doped tin oxide) conducting glass substrate, to achieve electron extraction and transport. We employed here thiolatedtruxene derivatives (20 nm thickness) on top of perovskite layer as HTMs. The entire fabrication procedure was in the open air at a common relative humidity of 45%. The fabricated perovskite devices were characterized by SEM (Figure 3) and PXRD (Figure S4).

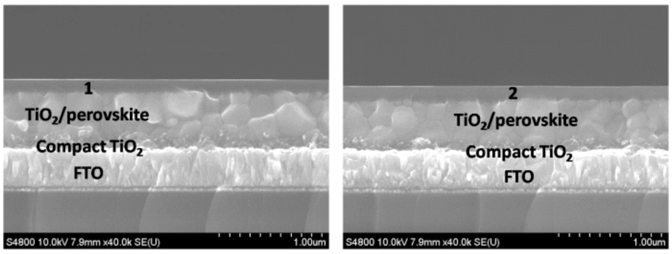

Figure 3. (1 &2) Cross-sectional SEM image of the device of FTO/TiO_2/Perovskite/Truxene derivatives film

To evaluate whether thiolatedtruxene derivatives could serve as effective materials to extract photogenerated holes from the perovskite layer, the *J−V* characteristics of FTO/TiO_2/$CH_3NH_3PbI_3$/Thiolatedtruxene/Au devices were measured under the illumination of AM 1.5, 100 mW cm^{-2}. As shown in Figure 4a, when ~80 nm thick thiolatedtruxene was deposited on the top of the perovskite layer as HTM, the best efficiency of compounds 1and 2 was achieved 11.45 % and 11.87 % respectively. The open-circuit voltage (V_{oc}), short-cut current (J_{sc}), and fill-factor (FF) were measured to be 0.97 V, 19.32 mA·cm^{-2}, and 61.12 % respectively for ethyl substituted thiolatedtruxene1 but in the case of butyl substituted thiolatedtruxene2 these values are little different 0.98 V, 19.43 mA·cm^{-2}, and 62.34 % (Table 2). The measurements over 30 devices gave an average efficiency of 10.8 ± 2.0% (Figure 4c). The incident photon-to-current conversion efficiency spectra (IPCE) of the device spanned from the UV region to 800 nm (Figure 4b), matching well with UV−vis absorption spectra of perovskite. Introducing different alkyl chain length (ethyl to butyl) in thiolatedtruxenederivates increase hydrophobicity of the HTM, which is readily provided as an effective molecular sealing approach to improve the stability of PSCs. Hydrophobic long chain alkylated thiolatedtruxene derivatives on perovskite surface immediately inhibite to enter water molecules into perovskite film and significantly enhance the stability of PSCs. The excellent performance of PSCs, involving the use of thiolatedtruxene as HTM, suggested a unique hole-extracting interface between perovskite and thiolatedtruxene. The higher efficiency also suggested the formation of Pb−S coordination-bond between thiolatedtruxene derivatives and perovskite. This work also re-established the concept for the formation of Pb−S coordination (ESI, Figure S5) bonds between thiolatedtruxene derivatives and perovskite that contribute the efficient electron extraction at the interface.

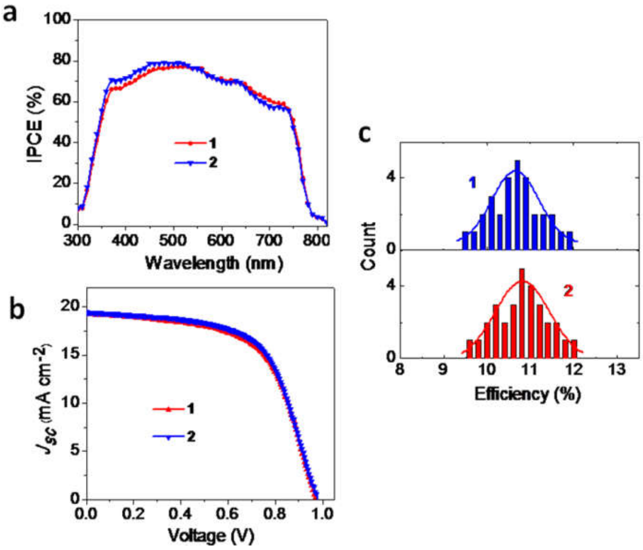

Figure 4. (a) Best I−V characteristics. (b) The IPCE spectra of the devices. (c) Comparison of the performance distributions of 30 individual devices of the cells

Table 2. Photovoltaic parameters of the champion cells

HTM	J_{sc}/mA·cm^{-2}	V_{oc}/V	*FF*/%	η/%	*Rs*/Ω·cm^{-2}
1	19.32	0.97	61.12	11.45	11.31
2	19.43	0.98	62.34	11.87	11.28

EXPERIMENTAL PROCEDURE

Materials

All chemicals and reagents were used as received from chemical companies without any further purification. The CH_3NH_3I was synthesized and purified according to the literature method (Tsuji, 2012). To a stirred solution of methylamine in methanol (40 wt.%, 24 mL) was slowly added aqueous hydroiodic acid (57 wt.%, 25 mL) at 0 ^{0}C. After 2 h, the precipitate was collected by evaporation at 50 ^{0}C for 1 h. The as-obtained product was washed with diethyl ether three times and then finally dried at 60 ^{0}C in a vacuum oven for 24 h to afford the desired pure CH_3NH_3I as white crystals. The starting compounds 4a, 4b, 5a and 5b was synthesized according to the literature method (Goubard, 2015 and Lor, 2001).

(5,5,10,10,15,15-hexaethyl-10,15-dihydro-5H-diindeno[1,2-a:1',2'-c]fluorene-2,7,12-triyl) tris(phenylsulfane) (1): Thiol (0.09 mL, 0.885 mmol) is added to a solution of sodium tert-butoxide (92.70 mg, 0.965 mmol) in 1.0 mL THF under nitrogen. This reaction mixture is stirred at 25 ^{0}C for 10 min. At this time, a solution of $ZnCl_2$ (70.14 mg, 0.515 mmol) in 1 mL of THF is added and the mixture is stirred for an additional 10 min. The desired aryl halide 5a (200 mg, 0.268 mmol) is added followed by a solution of LiI (53.81mg, 0.40 mmol) in 1 mL of THF, and a solution of the catalyst $[Pd(OAc)]_2$ (3.6 mg, 0.016 mmol), and PPh_3 (5.06 mg, 0.019mmol) in 0.5 mL of THF. This reaction is stirred at 80 ^{0}C for 12 h. The dark solution was poured into a separatory funnel. The layers were separated, and the aqueous phase was diluted with water (10 mL) and extracted with DCM (3 X 10 mL). The solution was dried over Na_2SO_4, and the solvents were removed under reduced pressure to give the crude products. The crude product was purified by column chromatography on silica gel using petroleum ether or mixtures of petroleum ether and CH_2Cl_2 (9:1) as eluent to give the title compound 1 (white solid, 180 mg, 80%). ^{1}H NMR (500 MHz, $CDCl_3$): δ 8.17 (d, 3H, J = 8.5 Hz), 7.98 (d, 3H, J = 2.0 Hz), 7.53 (d, 3H, J = 8.0 Hz), 7.51 (d, 6H, J = 8.0 Hz), 7.32-7.29 (m, 6H), 7.23 (t, 3H, J = 7.5 Hz), 2.95-2.88 (m, 6H), 2.15-2.07 (m, 6H), 0.22 (t, 18H, J = 7.0 Hz). ^{13}C NMR (125 MHz, $CDCl_3$): δ 155.2, 144.1, 139.3, 138.3, 137.2, 129.7, 129.2, 127.6, 127.3, 126.0, 125.8, 121.3, 57.3, 29.5, 8.6. ESI HRMS calcd (M+) 834.33210, found 834.3200.

(5,5,10,10,15,15-hexabutyl-10,15-dihydro-5H-diindeno[1,2-a:1',2'-c]fluorene-2,7,12-triyl)tris(phenylsulfane) (2): Thiol (0.07 mL, 0.719 mmol) is added to a solution of sodium tert-butoxide (75.41 mg, 0.78 mmol) in 1.0 mL THF under nitrogen. This reaction mixture is stirred at 25 ^{0}C for 10 min. At this time, a solution of $ZnCl_2$ (57.05 mg, 0.42 mmol) in 1 mL of THF is added and the mixture is stirred for an additional 10 min. The desired aryl halide 5b (200 mg, 0.218 mmol) is added followed by a solution of LiI (43.77 mg, 0.33 mmol) in 1 mL of THF, and a solution of the catalyst $[Pd(OAc)]_2$ (2.93 mg, 0.013mmol), and PPh_3 (4.12 mg, 0.016 mmol) in 0.5 mL of THF. This reaction is stirred at 80 ^{0}C for 12 h. The dark solution was poured into a separatory funnel. The layers were separated, and the aqueous phase was diluted with water (10 mL) and extracted with DCM (3 X 10 mL). The solution was dried over Na_2SO_4, and the solvents were removed under reduced pressure to give the crude products. The crude product was purified by column chromatography on silica gel using petroleum ether or mixtures of petroleum ether and CH_2Cl_2 (9:1) as eluent to give the title compound **2** (yellowish solid, 165 mg, 75%).^{1}H NMR (500 MHz, $CDCl_3$): δ 8.20 (d, 3H, J = 8.5 Hz), 7.58 (d, 3H, J = 2.0 Hz), 7.52 (d, 3H, J = 8.0 Hz), 7.50 (d, 6H, J = 8.5 Hz), 7.32-7.29 (m, 6H), 7.23 (t, 3H, J = 7.5 Hz), 2.90-2.84 (m, 6H), 2.08-2.02 (m, 6H), 0.97-0.83 (m, 12H), 0.58-0.50 (m, 6H), 0.46 (t, 18H, J = 7.5 Hz), 0.43-0.33 (m, 6H). ^{13}C NMR (125 MHz, $CDCl_3$): δ 156.0, 145.2, 139.0, 137.8, 137.2, 129.5, 129.2, 127.7, 127.3, 126.1, 125.7, 121.2, 56.1, 36.6, 26.6, 22.9, 13.9. ESI HRMS calcd (M+) 1002.52912, found 1002.5300.

Fabrication of Solar Cells: Fluorine-doped Tin Oxide (FTO) glass substrates with dimension of 2.0 cm × 2.0 cm were patterned by etching with zinc powder and 2 M hydrochloric acid. The substrates were then sequentially washed in ultrasonic baths of acetone, distilled water and ethanol. A compact TiO_2 blocking layer was spin-coated onto the cleaned FTO glass using 0.15 M Titanium tetraisopropanolate in ethanol solution at 2000 rpm for 30 s. The substrate was heated at 120 ^{0}C for 15 min, and then annealed at 550 ^{0}C for 30 min. After cooling to the room temperature, the film was immersed into the 20 mM $TiCl_4$ solution at 70 ^{0}C for 30 min. After dried, a ~200 nm thick mesoporous TiO_2 film was deposited on the pre-treated FTO substrate by spin-coating of the TiO_2 paste (Dyesol DSL 18NR-T) with ethanol (1:3, mass ratio), which was followed by the heating at 550 ^{0}C for 30 min. For the perovskite layer, the as-prepared substrate was infiltrated with a hot solution of PbI_2 in *N*, *N*-dimethylformamide (462 mg/1 mL) by spin-coating at 4000 rpm. for 30 s, and then dried at 120 ^{0}C for 5 min. After cooling to room temperature, the film was dipped into the solution of CH_3NH_3I in 2-propanol (10 mg/mL) for 30 s, which was spun at 4000 rpm for 20 s and then heated at 100 ^{0}C for 5 min. After the deposition of the perovskite layer, the Thiolatedtruxene compounds (Ethyl and butyl alkyl chain)/chlorobenzene (10 mg/mL) solution were coating by solution process at 4000 rpm for 30 s. Finally, a 80 nm thick Au counter electrode was deposited by thermal evaporation under reduced pressure of 2 × 10^{-7}Torr. The active area was 0.10 cm^{2}.

Device characterization: Current-voltage characteristics were recorded from a solar simulator equipped with a Keithley 2400 source meter and 300 W collimated Xenon lamp (Newport) calibrated with the light intensity to 100 mW cm^{-2} at AM 1.5 G solar light condition by the certified silicon solar cell. Incident photon-to-electron conversion efficiency (IPCE) was measured on a computer-controlled IPCE system (Newport) containing a Xenon lamp, a monochromator and a Keithleymultimeter. The system was calibrated with the certified silicon solar cell and the IPCE data were collected at DC mode. XRD patterns were analyzed by an X-ray diffractometer (Rigaku, RINT-2500) with a CuKa radiation source. The surface morphology of were recorded via a SEM-4800 field-emission scanning electron microscope (SEM). The UV-vis spectra were measured with the perovskite infiltrated mesoscopic TiO_2 films supported by FTO glass using a cary-5000 UV-vis spectrophotometer. The Time-resolved photoluminescence (PL) spectra were measured using an Edinburgh Instruments FLS920 spectrometer. The electrochemical impedance spectroscopy (EIS) was carried out in the frequency range from 10^{6} to 0.1 Hz in the dark, in which the potential bias was applied from 400 to 900 mV. According to the simplified transmission line model, the arcs at high-intermediate frequency can be supposed to be charge-transport resistance.

Conclusions

In summary, we report an efficient synthesis of two thiolatedtruxene-based two-dimensional HTMs, comprising electron-rich thiol engineered substituents. HTMs are obtained from simple and inexpensive starting materials merely in four scalable synthetic steps, offering potentially much lower production costs. Thiolatedtruxene derivatives exhibit surface interaction with perovskite material resulting in efficient hole injection from the valence band of perovskite into the HOMO of HTM. Power conversion efficiency of ~12.0 % was realized when 1 and 2 were used as HTM. Our study demonstrates a potential of two-dimensional materials like thiolatedtruxene derivatives as an alternative for the existing cost ineffective and synthetically challenging spiro- OMeTAD and PTAA HTMs in PSCs. We expect that further modification of the thiolatedtruxene core by molecular engineering of functional groups not only improves interfacial properties and efficiency but also protects from humidity and UV induced degradation of PSCs.

Acknowledgements

Dr. A. Pradhan acknowledges DST-INSPIRE Faculty project (DST/INSPIRE/04/2015/002294) and 2011-*i*ChEM-center, Xiamen University, China. A. P. acknowledges Ru-Qiang Lu, Xiaojing Jing,Dr. Xiao-Yu Cao and Prof. Nanfeng Zheng from State Key Laboratory of Physical Chemistry for Solid Surfaces, College of Chemistry and Chemical Engineering and Xiamen University, Xiamen (P. R. China) for discussions.

REFERENCES

Ahn, N., D. Y. Son, I. H. Jang, S. M. Kang, M. Choi, N. G. Park, 2015. *J. Am. Chem. Soc.* 137, 8696.

Bura,T., Leclerc, N., Fall, S., Leveque,P., Heiser, T., Ziessel, R. 2011. *Org. Lett.*13, 6030.

Bura,T., N. Leclerc, S. Fall, P. Leveque, T. Heiser, R. Ziessel, 2011.*Org. Lett.*13, 6030.

Cao, J., Y. M. Liu, X. Jing, J. Yin, J. Li, B. Xu, Y. Z. Tan, N. Zheng, 2015. *J. Am. Chem. Soc.* 137, 10914.

Goubard, F. and F. Dumur, 2015.*RSC Adv.*, *5*, 3521.

Hernandez, A. B., U. K. Pandey, E. Cavero, R. Termine, E. M. G. Frutos, J. L. Serrano, A. Golemme, B. G. Lor, 2013. Chem. Mater. 25, 117.

Im, J. H., C. R. Lee, J. W. Lee, S. W. Park, N. G. Park, 2011.*Nanoscale.,3*, 4088.

Im, J. H., Lee, C. R., Lee, J. W., Park, S. W., Park, N. G. 2011. Nanoscale 3, 4088.

Jeon, N. J., H. G. Lee, Y. C. Kim, J. Seo, J. H. Noh, J. Lee, S. Seok*, 2014.J. Am. Chem. Soc*136, 7837.

Jeon, N. J., J. H. Noh, W. S. Yang, Y. C. Kim, S. Ryu, J. Seo, S. I. Seok, 2015. Nature 517, 476.

Jeon, N. J., J. H. Noh, Y. C. Kim, W. S. Yang, S. Ryu, S. I. Seok, 2014. Nat. Mater. 6, 897.

Jeon, N. J., J. Lee, J. H. Noh, M. K. Nazeeruddin, M. Gratzel, S. I. Seok, J. Am. Chem. Soc. 135 (2013) 19087.

Kim, H. S., Lee, C. R., Im, J. H., Lee, K. B., Moehl, T., Marchioro, A.., Moon, S. J., Baker, R. H., Yum, J. H., Moser, J. E., Gratzel, M., Park, N. G. 2012. *Sci. Rep.* 2, 1.

Kojima, A., Teshima, K., Shirai, Y., Miyasaka, T. 2009. *J. Am. Chem. Soc.*131.,6050.

Lai, W. Y., Q. Y.He, R. Zhu, Q. Q. Chen, W. Huang, 2008. Adv. Funct. Mater.18, 265.

La-o-vorakiat,C., T. Salim, J. Kadro, M. T. Khuc, R. Haselsberger, L. Cheng, H. Xia, G. G. Gurzadyan, H. Su, Y. M. Lam, R. A. Marcus, M. E. M. Beyerle, E. E. M. Chia, 2015. Nat. Commun. 6, 7903.

Lee, M. M., J. Teuscher, T. Miyasaka, T. N. Murakami, H. J. Snaith, 2012. *Science* 338, 643.

Li, H., K. Fu, A. Hagfeldt, M. Gratzel, S. G. Mhaisalkar, A. C. GrimsdaleAngew. 2014. Chem. Int. Ed. 53, 4085.

Lim, K., M. S. Kang, Y. Myung, J. H. Seo, P. Banerjee, T. J. Marks, J. Ko, 2016. *J. Mater. Chem.*A, 4, 1186.

Liu, L., A. Mei, T. Liu, P. Jiang, Y. Sheng, L. Zhang, H. Han, 2015. *J. Am. Chem. Soc.* 137, 1790.

Lor, B. G., O. D. Frutos, P. A. Ceballos, T. Granier, A. M. Echavarren, 2001. *Eur. J. Org. Chem.* 2107.

Lv, S., L. Han, J.Xiao, L. Zhu, J. Shi, H. Wei, Y. Xu, J. Dong, X. Xu, D. Li, S. Wang, Y. Luo, Q. Meng, X. Li, 2014. Chem. Commun. 50, 6931.

Manser,J. S., P. J. Kamat, 2014. Nat. Photonics 8.,737.

Mei, A., X. Li, L. Liu, Z. Ku, T. Liu, Y. Rong, M. Xu, M. Hu, J. Chen, Y. Yang, M. Grätzel, H. Han, 2014. Science 345 295.

Min, J., Z. G. Zhang, Y. Hou, C. O. R. Quiroz, T. Przybilla, C. Bronnbauer, F. Guo, K. Forberich, H. Azimi, T. Ameri, E. Spiecker, Y. Li, C. Brabec, 2015. *J. Chem. Mater.*27, 227.

Nie, W., H. Tsai, R. Asadpour, J. C. Blancon, A. J. Neukirch, G. Gupta, J. J. Crochet, M. Chhowalla, S. Tretiak, M. A. Alam, H. L. Wang, A. D. Mohite, 2015. Science 347, 522.

Rakstys, K., A. Abate, M. I. Dar, P. Gao, V. Jankauskas, G. Jacopin, E. Kamarauskas, S. Kazim, S. Ahmad, M. Grätzel, M. K. Nazeeruddin, 2015. *J. Am. Chem. Soc.* 137, 16172.

Ramos, F. J. K. Rakstys, S. Kazim, M. Gratzel, M. K. Nazeeruddin, S. Ahmad, 2015. RSC Adv. 5, 53426.

Shao, J., Z. Guan, Y. Yan, C. Jiao, Q. H. Xu, C. Chi, 2011. *J. Org. Chem.* 76, 780.

Shelton, S. W., T. L. Chen, D. E. Barclay, B. Ma, 2012. ACS Appl. Mater. Interfaces 4, 2534.

Tsuji, H. Y. Ota, S. Furukawa, C. Mitsui, Y. Sato, E. Nakamura, 2012. *Asian J. Org. Chem.*,1, 34.

Wang,J., S. Wang, X. Li, L. Zhu, Q. Meng, Y. Xiao, D. Li, 2014. Chem. Commun. 50, 5829.

Xiao, M., F. Huang, W. Huang, Y. Dkhissi, Y. Zhu, J. Etheridge, A. G. Weale, U. Bach, Y. B. Cheng, L. Spiccia, 2014. Angew.Chem. Int. Ed. 53, 9898.

Xiao, Y., G. Han, Y. Chang, H. Zhou, M. Li, Y. Li, 2014. J. *Power Sources* 267, 1.

Yamada, Y.M, T. Nakamura, M. Endo, A. Wakamiya and Y. Kanemitsu, 2014. *J. Am. Chem. Soc.* 136, 11610.

Yang, W. S., J. H. Noh, N. J. Jeon, Y. C. Kim, S. Ryu, J. Seo, S. I. Seok, 2015. Science 348, 1234.

Zhou, H., Q. Chen, G. Li, S. Luo, T. B. Song, H. S. Duan, Z. Hong, J. You, Y. Liu, Y. Yang, Science, 345 (2014) 542.

Zuo, L., Z. Gu, T. Ye, W. Fu, G. Wu, H. Li, H. 2015. *Chen, J. Am. Chem. Soc.* 137. 2674.

****